

This discussion paper is/has been under review for the journal *Atmospheric Chemistry and Physics (ACP)*. Please refer to the corresponding final paper in *ACP* if available.

**Eurasian $^{14}\text{CO}_2$
measurements**

J. C. Turnbull et al.

Spatial distribution of $\Delta^{14}\text{CO}_2$ across Eurasia: measurements from the TROICA-8 expedition

J. C. Turnbull¹, J. B. Miller^{2,3}, S. J. Lehman¹, D. Hurst^{2,3}, P. P. Tans², J. Southon⁴,
S. Montzka², J. Elkins², D. J. Mondeel², P. A. Romashkin⁵, N. Elansky⁶, and
A. Skorokhod⁶

¹INSTAAR and Dept. of Geological Sciences, University of Colorado, Boulder, Colorado, USA

²NOAA/ESRL, 325 Broadway, Boulder, CO 80303, USA

³CIRES, University of Colorado, Boulder, Colorado, USA

⁴Department of Earth System Science, University of California, Irvine, USA

⁵NCAR, 1850 Table Mesa Dr, Boulder, CO 80307, USA

⁶A. M. Obukhov Institute of Atmospheric Physics RAS, Moscow, Russia

Received: 7 May 2008 – Accepted: 29 May 2008 – Published: 11 August 2008

Correspondence to: J. C. Turnbull (jocelyn.turnbull@colorado.edu)

Published by Copernicus Publications on behalf of the European Geosciences Union.

Title Page

Abstract

Introduction

Conclusions

References

Tables

Figures

◀

▶

◀

▶

Back

Close

Full Screen / Esc

Printer-friendly Version

Interactive Discussion



Abstract

Because fossil fuel derived CO₂ is the only source of atmospheric CO₂ that is devoid of ¹⁴C, atmospheric measurements of Δ¹⁴CO₂ can be used to constrain fossil fuel emissions at local and regional scales. However, at the continental scale, atmospheric transport and other sources of variability in Δ¹⁴CO₂ may influence the fossil fuel detection capability. We present a set of Δ¹⁴CO₂ observations from the train-based TROICA-8 expedition across Eurasia in March–April 2004. Local perturbations in Δ¹⁴CO₂ are caused by easily identifiable sources from nuclear reactors and localized pollution events. The remaining data show an increase in Δ¹⁴CO₂ from Western Russia (40° E) to Eastern Siberia (120° E), consistent with depletion in ¹⁴CO₂ caused by fossil fuel CO₂ emissions in heavily populated Europe, and gradual dispersion of the fossil fuel plume across Northern Asia.

Other tracer gas species which may be correlated with fossil fuel CO₂ emissions, including carbon monoxide, sulphur hexafluoride, and perchloroethylene, were also measured and the results compared with the Δ¹⁴CO₂ measurements. The sulphur hexafluoride longitudinal gradient is not significant relative to the measurement uncertainty. Carbon monoxide and perchloroethylene show large-scale trends of enriched values in Western Russia and decreasing values in Eastern Siberia, consistent with fossil fuel emissions, but exhibit significant spatial variability, especially near their primary sources in Western Russia.

The clean air Δ¹⁴CO₂ observations are compared with simulated spatial gradients from the TM5 atmospheric transport model. We show that the change in Δ¹⁴CO₂ across the TROICA transect is due almost entirely to emissions of fossil fuel CO₂, but that the magnitude of this Δ¹⁴CO₂ gradient is relatively insensitive to modest uncertainties in the fossil fuel flux. In contrast, the Δ¹⁴CO₂ gradient is strongly sensitive to the modeled representation of vertical mixing, suggesting that Δ¹⁴CO₂ may be a useful tracer for training mixing in atmospheric transport models.

Eurasian ¹⁴CO₂ measurements

J. C. Turnbull et al.

Title Page

Abstract

Introduction

Conclusions

References

Tables

Figures

◀

▶

◀

▶

Back

Close

Full Screen / Esc

Printer-friendly Version

Interactive Discussion



1 Introduction

Fossil fuel derived carbon dioxide (CO_2) is entirely devoid of radiocarbon (^{14}C) as a result of radioactive decay mean lifetime=8 267 y (Godwin, 1962) whereas other sources of CO_2 to the atmosphere contain ^{14}C at near ambient atmospheric concentrations.

Thus, precise measurements of the radiocarbon content of atmospheric CO_2 ($\Delta^{14}\text{CO}_2$) provide an excellent tracer for recently added fossil fuel CO_2 . The expected signal, expressed as a deviation from a globally well-mixed background value, is -2.8 permil (‰) in $\Delta^{14}\text{CO}_2$ for each part per million (ppm) of fossil fuel CO_2 added (Turnbull et al., 2006). $\Delta^{14}\text{CO}_2$ has been applied successfully as a fossil fuel CO_2 tracer at the local and regional scales where fossil fuel contributions are relatively large and uncertainties associated with atmospheric transport can be ignored (Turnbull et al., 2006; Levin et al., 2003; Meijer et al., 1996; Zondervan and Meijer, 1996). However, if the approach is to be successfully applied at larger spatial scales, all potential sources of $\Delta^{14}\text{CO}_2$ variability and their transport must be considered.

Previous studies of the time evolution of $\Delta^{14}\text{CO}_2$ (Levin and Kromer, 2004; Levin and Kromer, 1997; Manning et al, 1990; Nydal et al., 1983) have shown that production of ^{14}C from atmospheric nuclear weapons testing (“bomb ^{14}C ”) led to a near doubling of atmospheric $^{14}\text{CO}_2$ in the early 1960s (Levin et al., 1985), an increase of 900‰ in $\Delta^{14}\text{CO}_2$. Following the cessation of most atmospheric nuclear weapons testing in 1963 ongoing isotopic exchange with the oceans and terrestrial biosphere has reduced $\Delta^{14}\text{CO}_2$ of the atmosphere to near pre-bomb values. However, because of the relatively short residence time of carbon in the biosphere (about 10 years), the biosphere is now believed to be slightly enriching the atmosphere in $^{14}\text{CO}_2$ (Randerson et al., 2002). The initially very large disequilibrium between the oceans (and to a lesser extent, the terrestrial biosphere) dominated the secular decrease (and seasonal change) in $\Delta^{14}\text{CO}_2$ until the mid-1980s, causing annual decreases in $\Delta^{14}\text{CO}_2$ of up to 100‰. Since then, equilibration between the atmosphere and surface reservoirs has reduced the secular trend to just $\sim 5\% \text{ yr}^{-1}$ (Turnbull et al., 2007; Randerson et al., 2002). Fos-

Eurasian $^{14}\text{CO}_2$ measurements

J. C. Turnbull et al.

Title Page

Abstract

Introduction

Conclusions

References

Tables

Figures

◀

▶

◀

▶

Back

Close

Full Screen / Esc

Printer-friendly Version

Interactive Discussion



**Eurasian ^{14}C
measurements**

J. C. Turnbull et al.

sil fuel CO_2 emissions, which are currently about 7.5 Gt C yr^{-1} globally (Marland et al., 2003) and are entirely devoid of ^{14}C , would alone cause a globally averaged decrease in $\Delta^{14}\text{CO}_2$ of about $10\% \text{ yr}^{-1}$. Thus, fossil fuel emissions now dominate the observed secular change, but contributions to $\Delta^{14}\text{CO}_2$ from other sources may complicate the interpretation of the spatial distribution.

The gross disequilibrium flux of ^{14}C -depleted CO_2 from the ocean (due to radioactive decay in the slowly overturning oceans) to the atmosphere is comparable in magnitude to the flux of ^{14}C -free CO_2 from fossil fuel burning and is thus expected to have a comparable influence on global $\Delta^{14}\text{CO}_2$ (see Sect. 2.3). However, the impact on fossil fuel CO_2 detection using $\Delta^{14}\text{CO}_2$ over land is likely to be small because the fossil fuel and ^{14}C -depleted ocean sources are geographically separated, with the fossil fuel source almost entirely confined to the Northern Hemisphere land regions and the ocean contribution predominantly in the Southern Hemisphere (Randerson et al., 2002). Natural cosmogenic production and radioactive decay of ^{14}C in the troposphere are also unlikely to degrade the $\Delta^{14}\text{CO}_2$ fossil fuel detection capability significantly, since production has a nearly uniform zonal distribution, and decay in the troposphere decreases $\Delta^{14}\text{CO}_2$ by only about $0.1\% \text{ yr}^{-1}$. Exchange with the (^{14}C enriched) stratosphere may produce $\Delta^{14}\text{CO}_2$ anomalies in the upper troposphere, but the impact of this is likely small within the continental boundary layer (hereafter, CBL), due to the vertical distance from the tropopause to the CBL and the relatively slow vertical mixing of the CBL with the free troposphere. Gross biospheric exchange and the nuclear reactor ^{14}C source do affect the CBL and thus need to be accounted for.

While there have been numerous studies of the temporal change in $\Delta^{14}\text{CO}_2$, only a few observations of the synoptic spatial distribution have been made (Hsueh et al., 2007; Rozanski et al., 1995). Here we present $\Delta^{14}\text{CO}_2$ results from a transect across Russia from Moscow (55° N , $37^\circ 33' \text{ E}$) to Khabarovsk ($48^\circ 33' \text{ N}$, $135^\circ 6' \text{ E}$) as part of the Trans-Siberian Observations Into the Chemistry of the Atmosphere 8 (TROICA-8) expedition from 19 March–1 April 2004. These observations represent a transect

[Title Page](#)[Abstract](#)[Introduction](#)[Conclusions](#)[References](#)[Tables](#)[Figures](#)[◀](#)[▶](#)[◀](#)[▶](#)[Back](#)[Close](#)[Full Screen / Esc](#)[Printer-friendly Version](#)[Interactive Discussion](#)

through a large expected longitudinal $\Delta^{14}\text{CO}_2$ gradient as European fossil fuel CO_2 emissions are dispersed by the westerly air stream across Eurasia. We examine the spatial distribution of $\Delta^{14}\text{CO}_2$ for this region, and the impact of the various sources on it, showing that fossil fuel CO_2 emissions must be the dominant control on the observed spatial gradient.

Several trace gas species have been used or proposed as fossil fuel CO_2 tracers, based on estimates of the ratio of tracer to CO_2 emissions (which may vary in space and time) and assuming co-location of the tracer and fossil fuel CO_2 sources. Such tracers have the advantage over $\Delta^{14}\text{CO}_2$ in ease and lower cost of measurement, although their empirical correlation with fossil fuel CO_2 emissions appears to be weaker than for $\Delta^{14}\text{CO}_2$ (Turnbull et al., 2006). We therefore compare measurements of the prospective tracers carbon monoxide (CO), sulphur hexafluoride (SF_6), perchloroethylene (PCE) and chloroform with the $\Delta^{14}\text{CO}_2$ observations in order to evaluate their performance on the continental scale.

We also compare our observations to atmospheric $\Delta^{14}\text{CO}_2$ simulated by the TM5 atmospheric transport model (Krol et al., 2005). This allows us to test the consistency of model transport and emissions with our observations. As large-scale fossil fuel emissions are believed to be known within 10–15% (Marland et al., 2006), differences between simulated and observed $\Delta^{14}\text{CO}_2$ are more likely to result from model representation of atmospheric transport. In particular, the parameterization of vertical mixing is a major uncertainty in atmospheric transport models (Yang et al., 2007; Stephens et al., 2007; Peters et al., 2004; Denning et al., 1999) and we therefore evaluate the impact of changing vertical diffusion on the modeled $\Delta^{14}\text{CO}_2$ horizontal gradient. We also test the sensitivity of the simulated east-west gradient to the magnitude of European fossil fuel emissions.

Eurasian $^{14}\text{CO}_2$ measurements

J. C. Turnbull et al.

Title Page

Abstract

Introduction

Conclusions

References

Tables

Figures

I◀

▶I

◀

▶

Back

Close

Full Screen / Esc

Printer-friendly Version

Interactive Discussion



2 Methods

2.1 Sample collection and tracer concentration measurements

Air samples were obtained from an electric train based platform on the Trans-Siberian railway from Moscow (55°44' N, 37°33' E) to Khabarovsk (48°33' N, 135°6' E) between 19–24 March 2004 and the return journey from 27 March to 1 April 2004. The laboratory wagon was coupled directly behind the electric locomotive of a regular passenger train for the entire 8549 km (each way) journey. Outside air was drawn from the leading top edge of the laboratory wagon, about four meters above the rails, through 10 m of 6 mm OD Synflex tubing to a diaphragm pump. Samples were collected from this in 3L electro-polished stainless steel flasks by flushing for 10 min at 2–4 L min⁻¹ (flasks were fitted with inlet and exhaust valves, with the former including an internal dip tube to allow turbulent flushing of the flask interior) followed by filling to a pressure of 3 atmospheres over a fill time of about seven minutes (Crutzen et al., 1998).

These flasks were analyzed for multiple species, including several halocarbons, and these measurement methods are described elsewhere (Montzka et al., 1993; Belikov et al., 2006; Tarasova et al., 2006). $\Delta^{14}\text{CO}_2$ measurements were also made from these flasks and are described below.

In situ measurements of 12 different trace gas species, including CO and SF₆, were made using the four channel Airborne Chromatograph for Atmospheric Trace Species (ACATS-IV), using electron capture detection (Hurst et al., 2004; Romashkin et al., 2001). The measurement interval for the SF₆ (and N₂O) chromatographic channel was 70 sec, while CO (and CH₄, H₂) were assayed every 140 s. To compare with the flask measurements, we identified the in situ measurements made while each flask was filled. Typically, 2–3 in situ measurements of CO and 4–7 in situ measurements of SF₆ were made during each flask-filling period, and these were averaged to obtain a single data point. Uncertainties were assigned as the larger of the nominal measurement precision, or the one-sigma standard deviation of the averaged results.

Title Page

Abstract

Introduction

Conclusions

References

Tables

Figures

◀

▶

◀

▶

Back

Close

Full Screen / Esc

Printer-friendly Version

Interactive Discussion



2.2 $\Delta^{14}\text{CO}_2$ sample selection and measurement

In order to characterize the $\Delta^{14}\text{CO}_2$ signal arising from regional emissions and transport, samples with readily detectable contributions from local city sources must be identified and avoided. We used in situ CO measurements for this purpose, setting the local pollution threshold arbitrarily at 250 parts per billion (ppb) (compared to baseline values of CO for this transect varying from 227 ppb in the west to 156 ppb in the east). Only flasks corresponding with in situ CO measurements below 250 ppb were selected for $\Delta^{14}\text{CO}_2$ analysis (Fig. 1).

Methods for sample preparation, AMS measurement and uncertainty estimates are described in detail in Turnbull et al. (2007). Briefly, at the University of Colorado Laboratory for AMS Radiocarbon Preparation and Research, CO_2 was cryogenically extracted from the air samples and then split into two aliquots prior to reduction to graphite. Each graphite sample typically contained 0.6 mg C, and was analyzed for ^{14}C content at the University of California, Irvine accelerator mass spectrometry (AMS) facility. Results are reported as $\Delta^{14}\text{C}$, the per mil deviation of the sample ^{14}C content from the absolute radiocarbon standard, corrected for isotopic fractionation and radioactive decay (Stuiver and Polach, 1977). Single sample uncertainties range from 1.8‰ to 2.8‰, and are the larger of the reported AMS counting statistical uncertainty and the one-sigma standard deviation of repeated measurements of an in-house CO_2 -in-air standard. Of the 23 flasks collected, 20 were replicated; the pair differences are shown in Fig. 2. The single-sample uncertainties appear to be consistent with the observed pair differences (the normalized chi-squared value is 1.34, note that in the case where the uncertainties vary from sample to sample, the chi-squared test is a better test of the uncertainties than the root mean square). In one case, we measured $\Delta^{14}\text{CO}_2$ in four simultaneously collected flasks, and there is no significant difference between the four results.

Empirical evidence has suggested that undried CO_2 measurements from stainless steel flasks may be biased high, on the order of 1 ppm (T. Conway, personal communication). Qualitative comparison with CO_2 measurements on glass flasks collected

Title Page

Abstract

Introduction

Conclusions

References

Tables

Figures

◀

▶

◀

▶

Back

Close

Full Screen / Esc

Printer-friendly Version

Interactive Discussion



during the same expedition, but not at the same times, suggests that CO_2 values in the stainless steel flasks are enriched in CO_2 by less than 2 ppm (versus the atmospheric CO_2 loading of 383 ppm in spring 2004 at high northern latitudes (Tans and Conway, 2005)). This amount of CO_2 is unlikely to alter $\Delta^{14}\text{CO}_2$ by more than 0.5‰ (even assuming a 100‰ $\Delta^{14}\text{CO}_2$ difference between the flask CO_2 source and the atmospheric sample), substantially smaller than the measurement uncertainty.

2.3 TM5 model description

We compare the TROICA $\Delta^{14}\text{CO}_2$ observations with two model runs of the TM5 atmospheric transport model in which we have specified and transported CO_2 and $^{14}\text{CO}_2$ emissions. Model resolution is $4^\circ \times 6^\circ$, with 25 vertical layers, and the model is sampled at three hourly resolution to allow comparison with observations. CO_2 fluxes are composed of net oceanic fluxes derived from $\Delta p\text{CO}_2$ (Takahashi et al., 2002) and net fluxes from the terrestrial biosphere taken from the CASA biogeochemical model (Gurney et al., 2002). Annual global total fossil fuel CO_2 emissions are from Marland et al. (2006) until 2003 and linearly extrapolated to 2004. Fluxes are spatially distributed according to the EDGAR inventories (<http://www.rivm.nl/edgar/>; Olivier and Berdowski, 2001) using $1^\circ \times 1^\circ$ maps from 1995 and 2000 and extrapolating the emission pattern up to 2004. Additionally, a seasonal cycle based on the Blasing et al. (2005) analysis for the United States, which has $\sim 20\%$ higher emissions in winter than in summer, is imposed on the global emissions.

The modeled $^{14}\text{CO}_2$ budget is defined as

$$^{14}\text{CO}_{2(\text{modeled})} = ^{14}\text{CO}_{2\text{bg}} + ^{14}\text{CO}_{2\text{ff}} + ^{14}\text{CO}_{2\text{rh}} + ^{14}\text{CO}_{2\text{o}} + ^{14}\text{CO}_{2\text{cp}} \quad (1)$$

where $^{14}\text{CO}_{2(\text{modeled})}$ is the modeled result for a given grid point and $^{14}\text{CO}_{2\text{bg}}$ is the background atmospheric $^{14}\text{CO}_2$ concentration. $^{14}\text{CO}_{2\text{ff}}$ is the $^{14}\text{CO}_2$ value at that grid point due to fossil fuel emissions, and is, by definition, zero, as fossil fuels contain no ^{14}C . $^{14}\text{CO}_{2\text{rh}}$, $^{14}\text{CO}_{2\text{o}}$ and $^{14}\text{CO}_{2\text{cp}}$ are the heterotrophic respiration, ocean and

[Title Page](#)
[Abstract](#)
[Introduction](#)
[Conclusions](#)
[References](#)
[Tables](#)
[Figures](#)
[◀](#)
[▶](#)
[◀](#)
[▶](#)
[Back](#)
[Close](#)
[Full Screen / Esc](#)
[Printer-friendly Version](#)
[Interactive Discussion](#)


cosmogenic production ^{14}C sources and are described in detail below. $^{14}\text{CO}_2$ values are then combined with the separately transported total CO_2 values to obtain $\Delta^{14}\text{CO}_2$.

The $^{14}\text{CO}_2$ terrestrial disequilibrium-flux term is estimated using pulse-response functions from the CASA biosphere model (Thompson and Randerson, 1999) and the time history of atmospheric $\Delta^{14}\text{CO}_2$ (Levin and Kromer, 2004). The CASA pulse response functions are generated by allowing uptake of carbon for one year (as NPP) and then following its monthly release as heterotrophic respiration for 200 years. The result is an age distribution of heterotrophic respiration for each $1^\circ \times 1^\circ$ land region, which is then convolved with the atmospheric $\Delta^{14}\text{CO}_2$ history, to give the $\Delta^{14}\text{CO}_2$ of the respiratory flux. Given the terrestrial residence time of decades, we do not account for radioactive decay, resulting in a slight overestimate in the flux term (of less than 5%). The difference between the $\Delta^{14}\text{CO}_2$ of the respiratory flux and the current atmosphere is the disequilibrium which when multiplied by the heterotrophic respiration flux gives the disequilibrium flux, or gross biospheric $^{14}\text{CO}_2$ flux. For 2004, our estimated global total biospheric flux to the atmosphere is $370 \text{ mol } ^{14}\text{CO}_2 (3.9\% \text{ yr}^{-1} \text{ increase in } \Delta^{14}\text{CO}_2 \text{ if distributed globally})$, most of which is in the tropics. The gross ocean-to-atmosphere $^{14}\text{CO}_2$ flux is estimated using climatological surface ocean pCO_2 (Takahashi et al., 2002), an assembly of surface ocean $\Delta^{14}\text{C}$ of dissolved inorganic carbon (DIC) measurements from the GLODAP project (cdiac.ornl.gov/oceans/glodap/Glodap_home.htm), and the gas transfer formulation of Wanninkhof (1992). The flux is calculated on a monthly basis on a $4^\circ \times 5^\circ$ grid of ice-free ocean areas. We make special note that we use wind-speed data from 10 m above the surface. Compared to previously published results (e.g. Takahashi et al., 2002), which used the 0.995 sigma level winds ($\sim 40 \text{ m a.s.l.}$), using 10 m winds results in a less negative global disequilibrium flux, mainly due to lower wind speeds in the Southern Ocean. The calculated disequilibrium flux varies interannually, but only as a result of the changing atmosphere. Given that the GLODAP product is not a climatology, but instead consists of surface ocean measurements taken over more than a decade, there

Eurasian $^{14}\text{CO}_2$ measurements

J. C. Turnbull et al.

Title Page

Abstract

Introduction

Conclusions

References

Tables

Figures

◀

▶

◀

▶

Back

Close

Full Screen / Esc

Printer-friendly Version

Interactive Discussion



is no easy way of extrapolating the values to 2004. Nonetheless, it is likely that the dominant cause of changing disequilibrium is the atmospheric $\Delta^{14}\text{CO}_2$ and not the surface ocean values. For 2004, the estimated global total oceanic flux to the atmosphere is $-325 \text{ mol } ^{14}\text{CO}_2(-3.4\% \text{ yr}^{-1}$ if distributed globally), most of which is in the Southern Ocean.

Cosmogenic production of ^{14}C occurs in both the stratosphere and troposphere and the total production of 530 mole yr^{-1} is distributed horizontally with maximum production at the magnetic poles and a minimum at the equator as described by Masarik and Beer (1999). Production is scaled vertically to agree with vertical distribution estimates from Masarik and Beer (1999) and Lal (1988) such that there is a maximum near the tropopause with a nearly linear decay to zero production at the surface and 60 km, and with roughly equal production in the stratosphere and upper troposphere. This vertical distribution of production reflects the balance between cosmic ray flux, which attenuates from the top of the atmosphere, and atmospheric density.

Input meteorological driver data for TM5 is derived from the ECMWF model (www.ecmwf.int; Gibson et al., 1999), and for the simulations here, meteorology for March and April 2004 is used. TM5 transport is described more fully by Krol et al. (2004).

Production of $^{14}\text{CO}_2$ from the nuclear power industry is estimated to be $45\text{--}80 \text{ mol } ^{14}\text{C yr}^{-1}$ (equating to less than $1\% \text{ yr}^{-1}$ in $\Delta^{14}\text{CO}_2$ if distributed globally) (UNSCEAR, 2000) and is ignored in the model, as it is small and there is considerable uncertainty in both the magnitude and temporal distribution. Ignoring this term introduces a small bias, especially in the temporal evolution of the modeled $\Delta^{14}\text{CO}_2$, and also means that we cannot expect our model simulation to reproduce observations influenced by nuclear reactor emissions near the TROICA route.

Net $^{14}\text{CO}_2$ fluxes into and out of the biosphere and ocean, and autotrophic respiration are not included because $\Delta^{14}\text{CO}_2$ accounts for natural fractionation (Stuiver and Polach, 1977) and these fluxes are therefore all necessarily zero.

For any given emissions at the surface, the model representation of trace gas concentration within the CBL is expected to be sensitive to the strength of simulated or

Eurasian $^{14}\text{CO}_2$ measurements

J. C. Turnbull et al.

Title Page

Abstract

Introduction

Conclusions

References

Tables

Figures

◀

▶

◀

▶

Back

Close

Full Screen / Esc

Printer-friendly Version

Interactive Discussion



[Title Page](#)[Abstract](#)[Introduction](#)[Conclusions](#)[References](#)[Tables](#)[Figures](#)[◀](#)[▶](#)[◀](#)[▶](#)[Back](#)[Close](#)[Full Screen / Esc](#)[Printer-friendly Version](#)[Interactive Discussion](#)

specified vertical mixing (i.e. ventilation of the CBL). Comparison of observed mixing ratios of both SF₆ (Peters et al., 2004; Denning et al., 1999) and CO₂ (Yang et al., 2007; Stephens et al., 2007) with their simulated values indicate that vertical mixing may be underestimated in some atmospheric transport models, including TM5. To examine this further, we use two different model constructions: (a) the standard TM5 vertical mixing scheme (TM5std), which includes parameterization of convection and vertical diffusion (Krol et al., 2004); and (b) a “fast mixing” scheme (TM5fast), where surface emissions are nearly instantaneously mixed up to the height of the model boundary layer. In the latter, vertical diffusion below the height of the model boundary layer is set to 1000 m²s⁻¹, compared to typical values of order 50 m² s⁻¹ (mid-day, summer) and <1 m² s⁻¹ (night). This fast mixing scheme is not intended to present a realistic mixing scheme, but rather is a simple implementation of mixing to test for differences (Peters et al., 2004).

3 Results and discussion

3.1 Δ¹⁴CO₂ results

The results for 22 sampling locations between 37° E and 124° E are shown in Fig. 3 (including one location where two pairs of flasks were collected simultaneously), of which 18 locations were sampled on the eastbound transect from 19–24 March 2004, and four locations on the return, westbound, transect from 27 March–1 April 2004. The eastbound and westbound observations are not statistically distinguishable (the linear longitudinal trends are statistically indistinguishable at the 90% confidence level) and we therefore treat both transects as a single dataset. The latitude ranges from 58.5° N in the west to 51.5° N in the east (Fig. 4). The Δ¹⁴CO₂ results display considerable longitudinal variability, much of which is probably attributable to two local effects: ¹⁴C enrichment due to emissions from nuclear power plants, and highly-efficient fossil fuel pollution sources that emit ¹⁴C-free CO₂, but very little CO.

**Eurasian ^{14}C
 CO_2
measurements**

J. C. Turnbull et al.

While global production of ^{14}C in nuclear power plants is small compared to other ^{14}C sources (increasing the global mean $\Delta^{14}\text{CO}_2$ by less than $1\% \text{ yr}^{-1}$), substantial local $^{14}\text{CO}_2$ enrichments may occur close to nuclear power plants. The magnitude of the $^{14}\text{CO}_2$ source is dependent on the reactor type, with pressurized water reactors (PWR) predominantly producing ^{14}C as $^{14}\text{CH}_4$, whereas other reactor types, including boiling water reactors (BWR) and the Russian RBMK light-water cooled, graphite-moderated reactors produce ^{14}C mostly as $^{14}\text{CO}_2$ (UNSCEAR, 2000). $\Delta^{14}\text{CO}_2$ values 50–300% over background have been measured within 2 km of two German BWR reactors (Levin et al., 1988) and plant material around the Ignalina, Lithuania RBMK reactor is elevated by up to 20 000%, with typical values 250% above background (Magnusson et al., 2004). In order to screen for such local enrichments we used the HYSPLIT back-trajectory model (Draxler and Rolph, 2003), obtaining back-trajectories for each sampling location and time (Fig. 4). From this, we identified three samples that received air that may have been influenced by local nuclear reactor effluent (excluding PWR reactors which should not affect $\Delta^{14}\text{CO}_2$ measurements). These flagged samples are excluded from further analysis.

Incursions of stratospheric air, which is enriched in ^{14}C by about 100% relative to the troposphere (Nakamura et al., 1994), may also produce anomalously high $\Delta^{14}\text{CO}_2$ values. Such incursions would also be expected to cause depletion in nitrous oxide (N_2O), methane (CH_4) and CO , which are all produced in the troposphere and destroyed in the stratosphere. In situ measurements of these three species do not indicate any significant depletions. We also examined the vertical component of the HYSPLIT back-trajectories, which do not indicate strong stratospheric incursions. We conclude that this process has not significantly influenced our dataset.

In order to obtain the regionally representative background signal, we avoid samples taken very close to localized fossil fuel sources. In selecting samples for measurement, we screened for high CO values to avoid obviously polluted samples. However, high efficiency combustion can produce fossil fuel CO_2 with very little accompanying CO emission (e.g. in the United States, power plants have very low CO emis-

[Title Page](#)[Abstract](#)[Introduction](#)[Conclusions](#)[References](#)[Tables](#)[Figures](#)[◀](#)[▶](#)[◀](#)[▶](#)[Back](#)[Close](#)[Full Screen / Esc](#)[Printer-friendly Version](#)[Interactive Discussion](#)

sions of 0.1 ppb CO/ppm CO₂; USEPA, 2004). Three samples were collected within 20 km of large population centers (Novosibirsk, population 1 200 000; Irkutsk, population 750 000; and Ulan-Ude, population 400 000) and these were flagged as potentially influenced by local pollution sources.

5 During the winter at 50–60° N latitude, biospheric respiration is small, but we estimate its impact as follows: the respiration $\Delta^{14}\text{C}$ value was assumed to be 120‰ (from a 10 year mean soil turnover time; Trumbore, 1997, and the atmospheric $\Delta^{14}\text{CO}_2$ history; Levin and Kromer, 2004), with a CO₂ flux of $0.5 \mu\text{mol m}^{-2} \text{s}^{-1}$ which was allowed to build up over several days within a boundary layer 1000 m deep. This results in
10 an increase in $\Delta^{14}\text{CO}_2$ in the boundary layer of less than 0.2‰. This estimate is in agreement with results from both of our model runs using the CASA biosphere model input (Randerson et al., 1997, described in Sect. 2.3), which indicate that respiration contributes less than 0.2‰ to the modeled $\Delta^{14}\text{CO}_2$ gradient, which is not significant relative to the ¹⁴C measurement uncertainties.

15 Biomass and biofuel combustion could also contribute to changes $\Delta^{14}\text{CO}_2$. Biomass combustion is usually less efficient than fossil fuel combustion, with emission ratios of 60–250 ppb CO/ppm CO₂ (Andreae and Merlet, 2001) so that we would expect to see high CO values if biomass combustion was contributing to CO₂ and hence to $\Delta^{14}\text{CO}_2$. We screened for CO values higher than 250 ppb, so that the maximum elevation in CO
20 is 80 ppb above the lowest CO value of 170 ppb observed during times when flasks were being filled for ¹⁴CO₂. Assuming a $\Delta^{14}\text{C}$ value of 120‰ for biomass combustion, and the most efficient combustion ratio of 60 ppb CO/ppm CO₂, the contribution from biomass burning to the $\Delta^{14}\text{CO}_2$ value is at most 0.2‰.

We noted earlier that the impact of ocean exchange on $\Delta^{14}\text{CO}_2$ over Eurasia is
25 expected to be small and that cosmogenic ¹⁴C production is distributed evenly by longitude. It follows then that since the local influences of nuclear reactor effluent can be easily identified, the remaining $\Delta^{14}\text{CO}_2$ observations must predominantly reflect the influence of fossil fuel emissions.

Figure 5 shows the “clean air” dataset (solid points, each point is the average of the

Eurasian ¹⁴CO₂
measurements

J. C. Turnbull et al.

Title Page

Abstract

Introduction

Conclusions

References

Tables

Figures

◀

▶

◀

▶

Back

Close

Full Screen / Esc

Printer-friendly Version

Interactive Discussion



**Eurasian $^{14}\text{CO}_2$
measurements**

J. C. Turnbull et al.

Title Page

Abstract

Introduction

Conclusions

References

Tables

Figures

◀

▶

◀

▶

Back

Close

Full Screen / Esc

Printer-friendly Version

Interactive Discussion



two measurements from that flask) along with the samples flagged as influenced by either nuclear reactor effluent or by local city pollution sources. We note two anomalously high values amongst the retained data, at 38°E and 106°E . These values may be simply due to statistical uncertainty, or may be due to real (but otherwise unidentified in our screening protocols) atmospheric variability in $\Delta^{14}\text{CO}_2$ values; in either case, these points are valid and must be considered in the remainder of our analysis.

$\Delta^{14}\text{CO}_2$ increases by $5.0 \pm 1.0\text{‰}$ across the transect from 40°E to 120°E (Fig. 5) and this difference is significant at the 99% confidence level. This is consistent with a (^{14}C -free) fossil fuel CO_2 source in the western part of the transect, which is gradually dispersed by atmospheric transport across Eurasia. The observed isotopic change implies a gradient of 1.8 ppm of fossil fuel derived CO_2 (assuming a -2.8‰ change in $\Delta^{14}\text{CO}_2$ per ppm of fossil fuel CO_2 added). $\Delta^{14}\text{CO}_2$ measurements from Niwot Ridge, Colorado, USA (NWR, 40.05°N , 105.58°W , 3475 m a.s.l.) are believed to represent relatively clean free tropospheric air over North America and, likely, the Northern Hemisphere mid-latitudes in general. NWR observations for 3 sampling dates during the time of the TROICA-8 campaign give a mean $\Delta^{14}\text{CO}_2$ value of $66.8 \pm 1.3\text{‰}$ (grey bar in Fig. 5) (Turnbull et al., 2007). The Eastern Siberian part of the TROICA transect shows values ($62.8 \pm 0.5\text{‰}$) most similar to the NWR value, consistent with an easterly dilution of the fossil fuel content in boundary layer air away from the primary source, but suggesting that some influence from the European fossil fuel CO_2 source remains in the Eastern Siberian air mass.

3.2 Comparison with correlate tracer species

CO is co-emitted with CO_2 during fossil fuel combustion, and if the emission ratio of CO to CO_2 (R_{CO}) is known, it can be used to estimate fossil fuel emissions (Levin and Karstens, 2007; Turnbull et al., 2006; Potosnak et al., 1999; Bakwin et al., 1997; Wofsy et al., 1994). In order to examine the potential correlation of measured CO with fossil fuel emissions, the CO observations made during the TROICA transect were compared with the $\Delta^{14}\text{CO}_2$ observations, using only those CO observations corresponding to the

time periods of samples in the cleaned $\Delta^{14}\text{CO}_2$ dataset (Fig. 6).

The CO observations show a decline in value from west to east, consistent with a CO source in the west being gradually diluted by mixing and CO destruction as the air mass moves eastwards. The longitudinal dependence of the CO observations is roughly the opposite of that for $\Delta^{14}\text{CO}_2$, and the slope of the relationship is -7.9 ± 1.9 ppb/‰, implying an R_{CO} value of 22.3 ± 5.3 ppb CO/ppm CO_2 (given -2.8% /ppm of fossil fuel CO_2). This is consistent with inventory-based estimates of R_{CO} for this region (Olivier and Berdowski, 2001). However, the correlation between the two species is not particularly strong ($r^2=0.44$, $p=0.005$). This may be due in part to difficulties in matching the sometimes rapidly varying CO measurements (made every 140 s) with the $\Delta^{14}\text{CO}_2$ measurements from flasks (collected over about seven min). The observations suggest that CO measurements can provide a reasonable estimate of fossil fuel emissions far from the source region, where atmospheric transport and mixing has resulted in a regionally representative emissions ratio. Close to the source region other sources of CO and/or variability in R_{CO} appear to confound the relationship between CO and fossil fuel CO_2 . We also note that the usefulness of CO as a tracer for fossil fuel CO_2 in Siberia is likely to be limited to winter and spring when destruction of CO by OH and production by biomass burning and biogenic hydrocarbon oxidation is low.

SF_6 , which is entirely anthropogenic and emitted to the atmosphere via leaks from electrical switching equipment, has also been used as a fossil fuel CO_2 tracer (Hurst et al., 2006; Bakwin et al., 1997). On regional scales, SF_6 does not appear to perform well as a fossil fuel CO_2 tracer, probably because SF_6 and fossil fuel CO_2 emissions are not well correlated in space (Turnbull et al., 2006; Rivier et al., 2006) (on larger scales, the assumption of co-location of SF_6 and fossil fuel CO_2 sources may have greater validity). There is no statistically significant east-west difference in the observations (Fig. 6c). The variation amongst the observations, which is ± 0.03 ppt at one-sigma, lies within measurement uncertainty of 0.06–0.09 ppt for this experiment. This also holds for the entire set of in situ SF_6 observations made during this transect (mean 5.59 ± 0.07 ppt), excluding 23 measurements in the vicinity of the city of Perm, where SF_6 is apparently

Eurasian $^{14}\text{CO}_2$ measurements

J. C. Turnbull et al.

Title Page

Abstract

Introduction

Conclusions

References

Tables

Figures

◀

▶

◀

▶

Back

Close

Full Screen / Esc

Printer-friendly Version

Interactive Discussion



produced. This is consistent with results from SF₆ observations during a previous TROICA transect in 1996 (Crutzen et al., 1998), but is in contrast to continental scale observations for North America for 2003, where much larger variability in SF₆ mixing ratios was observed (Hurst et al., 2006).

5 Perchloroethylene (1,1,2,2-tetrachloroethene, C₂Cl₄, "PCE") is widely used as a dry cleaning solvent, and has been used as a tracer for polluted air masses (Barnes et al., 2003; Gloor et al., 2001). It has been proposed as a tracer for fossil fuel CO₂ (Rivier et al., 2006; Wofsy et al., 1994), but has not been well evaluated for this purpose. Concentrations of PCE were measured in the same flask samples as the Δ¹⁴CO₂ measurements. The overall correlation between PCE and Δ¹⁴CO₂ is weak for this dataset ($r^2=0.16$, $p=0.13$, Fig. 6d), but is heavily influenced by a single outlier

The observed spatial pattern of PCE is nonetheless similar to that for CO, with very little variability and generally lower mixing ratios in the eastern part of the transect versus larger mixing ratios and variability in the west, near probable source areas. The two flasks with highest PCE values (13.1 and 13.5 ppt) also contain elevated levels of many other anthropogenic trace gases, including HCFC-22, HFC-134a, benzene and toluene (data not shown), implying that much of the variability in the western part of the transect may be due to local anthropogenic trace gas sources unrelated to fossil fuel sources.

20 Numerous halocarbon species were also measured in the same flasks. Since most of these species are anthropogenic, they may be useful as fossil fuel CO₂ tracers. Of the 27 species analyzed, only chloroform (trichloromethane, CHCl₃) shows any correlation consistent with a co-location with fossil fuel sources, at least in this data from Russia (data not shown). A larger dataset would be required to evaluate how consistent the chloroform source is, and whether it could be widely applied as a fossil fuel tracer.

[Title Page](#)[Abstract](#)[Introduction](#)[Conclusions](#)[References](#)[Tables](#)[Figures](#)[◀](#)[▶](#)[◀](#)[▶](#)[Back](#)[Close](#)[Full Screen / Esc](#)[Printer-friendly Version](#)[Interactive Discussion](#)

3.3 Comparison with atmospheric transport model

Simulated $\Delta^{14}\text{CO}_2$ values were extracted from the two TM5 model runs for grid cells and times corresponding to the TROICA samples, as well as those corresponding to NWR sampling times. The simulated NWR values are 67.0‰ and 67.4‰ for TM5std and TM5fast, respectively, in agreement with the observed NWR value of $66.8 \pm 1.3\%$ for the same time period.

The simulated $\Delta^{14}\text{CO}_2$ values for the TROICA transect are shown in Fig. 5. The westernmost sample, taken at 56.1° N, 37.9° E, appears to be influenced by model representation error, due to the very strong emissions from Moscow (population 8 000 000) which are injected into the same model gridbox. With a horizontal model resolution of $6 \times 4^\circ$, errors of this size near sources are not surprising. The modeled results are otherwise broadly consistent with the observed increase in $\Delta^{14}\text{CO}_2$ from west to east. The shape of the observed gradient is also well captured by the model, with the areas of steep gradient between 40–60° E and again from about 85–100° E, and flattening in the middle and far eastern regions of the transect. This is reflected in the good correlation between the observations and the modeled $\Delta^{14}\text{CO}_2$ values ($r=0.78$ and 0.81 for TM5std and TM5fast, respectively).

It is apparent from Fig. 7, where the contribution of each $^{14}\text{CO}_2$ source to the spatial gradient is shown individually, that the modeled spatial gradient is due almost entirely (90%) to fossil fuel CO_2 emissions. The oceans and cosmogenic production, as discussed earlier, contribute very little to the longitudinal gradient. There is greater variability in the terrestrial biospheric contribution, but overall it contributes only 0.1‰ to the gradient.

Despite the overwhelming influence of fossil fuel CO_2 emissions, the magnitude of the modeled gradient is only weakly sensitive to the modest uncertainties in the fossil fuel emissions flux. Increasing the global fossil fuel CO_2 emissions by 10% increased the modeled west-east gradient by only 0.2‰ in each model scenario. Similarly, when the model runs were repeated with seasonally flat fossil fuel emissions (but with the

Title Page

Abstract

Introduction

Conclusions

References

Tables

Figures

◀

▶

◀

▶

Back

Close

Full Screen / Esc

Printer-friendly Version

Interactive Discussion



same annual emission total), there was only a negligible difference in the modeled results. This is most likely due to the fact that in March and April the seasonally adjusted fossil fuel flux is very close to the annual mean values.

The magnitude of the west-east gradient is slightly overestimated in TM5std compared to the observations, by a factor of 1.2 ± 0.2 . This is consistent with a comparison of SF_6 observations from an earlier TROICA expedition (in 1996) with the TransCom suite of models, which indicated that most models, including the precursor of TM5 (TM3), overestimated the observed SF_6 longitudinal gradient, implying that the modeled vertical mixing was too slow (Denning et al., 1999). When unrealistically fast vertical mixing is applied, in the TM5fast simulation, the $\Delta^{14}\text{CO}_2$ values in the west, near the fossil fuel source, are about 2% lower than in TM5std, leading to a reduction in the simulated gradient of 35%, and slightly underestimating the observed gradient by a factor of 0.8 ± 0.1 .

These findings suggest that with sufficient observations, it may be possible to improve constraints on model vertical mixing parameterizations using $\Delta^{14}\text{CO}_2$ observations, providing a complementary diagnostic to SF_6 , which has previously been used for this purpose. While a much larger suite of SF_6 observations is available, $\Delta^{14}\text{CO}_2$ has the advantage of better-constrained source strength, with fossil fuel emissions being known to within 10–15% at the continental scale (Marland et al., 2003). In contrast, the SF_6 source distribution and strength is much less well constrained, especially for Russia, with uncertainties estimated to be 50% (Olivier et al., 2001).

4 Conclusions

We obtained a spatial distribution of $\Delta^{14}\text{CO}_2$ across Eurasia for March–April 2004. Local pollution sources of ^{14}C -free derived fossil fuel CO_2 and nuclear reactor produced $^{14}\text{CO}_2$ produce locally higher or lower $\Delta^{14}\text{CO}_2$ values, respectively. Use of back-trajectories allowed us to identify these locally influenced samples, and obtain a background continental boundary layer dataset for this region. The magnitude of the

Title Page

Abstract

Introduction

Conclusions

References

Tables

Figures

◀

▶

◀

▶

Back

Close

Full Screen / Esc

Printer-friendly Version

Interactive Discussion



Eurasian $^{14}\text{CO}_2$ measurements

J. C. Turnbull et al.

$\Delta^{14}\text{CO}_2$ gradient is consistent with the dispersion of fossil fuel CO_2 emissions produced in Europe, and atmospheric transport across northern Asia dispersing and diluting the fossil fuel plume.

Comparison of the $\Delta^{14}\text{CO}_2$ measurements with potential fossil fuel correlate tracer species shows that while several species may be useful fossil fuel tracers on large scales, they exhibit considerable variability in regions close to significant sources. This is likely because, in contrast to $\Delta^{14}\text{CO}_2$ which is directly related to the fossil fuel emissions, correlate tracer emissions may not be entirely co-located with the fossil fuel source. This variability must be accounted for if these correlate tracer species are to be used as fossil fuel tracers.

The $\Delta^{14}\text{CO}_2$ distribution simulated using TM5 shows gradients across the TROICA transect similar to that determined from the observations, and imply that the $\Delta^{14}\text{CO}_2$ gradient is almost entirely due to fossil fuel CO_2 . While the gradient is weakly sensitive to the (modest) uncertainty in fossil fuel emissions, changes in the model mixing parameterization result in much larger changes in the gradient, demonstrating the potential for $\Delta^{14}\text{CO}_2$ observations over the continents to constrain vertical mixing in atmospheric transport models.

Acknowledgements. The International Scientific and Technology Fund (ISTC, projects 2073 and 2070) and the Russian Basic Research Foundation (project 06-05-08089) supported the sampling campaign. Funding for $^{14}\text{CO}_2$ analysis was provided by NASA's Atmospheric Chemistry Modeling and Analysis Program (ACMAP) and Upper Atmospheric Research Program and from NOAA's Atmospheric Composition and Climate Program.

References

- Andreae, M. O. and Merlet, P.: Emission of trace gases and aerosols from biomass burning, *Glob. Biogeochem. Cy.*, 15(4), 955–966, 2001.
- Bakwin, P. S., Hurst, D. F., Tans, P. P., and Elkins, J. W.: Anthropogenic sources of halocarbons,

[Title Page](#)[Abstract](#)[Introduction](#)[Conclusions](#)[References](#)[Tables](#)[Figures](#)[◀](#)[▶](#)[◀](#)[▶](#)[Back](#)[Close](#)[Full Screen / Esc](#)[Printer-friendly Version](#)[Interactive Discussion](#)

Eurasian ¹⁴CO₂ measurements

J. C. Turnbull et al.

Title Page

Abstract

Introduction

Conclusions

References

Tables

Figures

◀

▶

◀

▶

Back

Close

Full Screen / Esc

Printer-friendly Version

Interactive Discussion



- sulfur hexafluoride, carbon monoxide, and methane in the southeastern United States, *J. Geophys. Res.*, 102(D13), 15 915–15 925, 1997.
- Barnes, D. H., Wofsy, S. C., Fehla, B. P., Gottlieb, E. W., Elkins, J. W., Dutton, G. S., and Montzka, S. A.: Urban/industrial pollution for the New York City – Washington D.C. corridor, 1996–1998: 1. Providing independent verification of CO and PCE emissions inventories, *J. Geophys. Res.*, 108(D6), 4185, 2003.
- Belikov, I., Brenninkmeijer, C. A. M., Elansky, N., and Ral'ko, A.: Methane, carbon monoxide, and carbon dioxide concentrations measured in the atmospheric surface layer over continental Russia in the TROICA experiments, *Izvestiya, Atmos. Ocean Phys.*, 42, 46–59, 2006.
- Blasing, T., Broniak, C., and Marland, G.: The annual cycle of fossil-fuel carbon dioxide emissions in the United States, *Tellus*, 57B, 107–115, 2005.
- Crutzen, P. J., Elansky, N., Hahn, M., Golitsyn, G., Brenninkmeijer, C. A. M., Scharffe, D., Belikov, I., Maiss, M., Bergamaschi, P., Rockmann, T., Grisenko, A., and Sevostyanov, V.: Trace gas measurements between Moscow and Vladivostok using the Trans-Siberian railroad, *J. Atmos. Chem.*, 29, 179–194, 1998.
- Denning, A. S., Holzer, M., Gurney, K. R., Heimann, M., Law, R. M., Rayner, P. J., Fung, I. Y., Fan, S., Taguchi, S., Friedlingstein, P., Balkanski, Y., Taylor, J., Maiss, M., and Levin, I.: Three-dimensional transport and concentration of SF₆: A model intercomparison study (TransCom 2), *Tellus*, 51B, 266–297, 1999.
- Draxler, R. and Rolph, G.: HYSPLIT (HYbrid Single-Particle Lagrangian Integrated Trajectory) Model access via NOAA ARL READY Website (<http://www.arl.noaa.gov/ready/hysplit4.html>), NOAA Air Resources Laboratory, Silver Spring, MD, 2003.
- Gibson, J., Kållberg, P., Uppala, S., Hernandez, A., Nomura, A., and Serrano, E.: ERA-15 description, in ECMWF Re-analysis Project Report Series, Centre europeen por les previsions meteorologique a moyen terme, 1999.
- Gloor, M., Bakwin, P. S., Hurst, D. F., Lock, L., Draxler, R., and Tans, P. P.: What is the footprint of a tall tower?, *J. Geophys. Res.*, 106(D16), 17 831–17 840, 2001.
- Godwin, H.: Half-life of radiocarbon, *Nature*, 195, 984, 1962.
- Gurney, K. R., Law, R. M., Denning, A. S., Rayner, P. J., Baker, D., Bousquet, P., Bruhwiler, L., Chen, Y.-H., Ciais, P., Fan, S., Fung, I. Y., Gloor, M., Heimann, M., Higuchi, K., John, J., Maki, T., Maksyutov, S., Masarie, K. A., Peylin, P., Prather, M., Pak, B. C., Randerson, J., Sarmiento, J. L., Taguchi, S., Takahashi, T., and Yuen, C.-W.: Towards robust regional estimates of CO₂ sources and sinks using atmospheric transport models, *Nature*, 415, 626–

630, 2002.

Hsueh, D. Y., Krakauer, N. Y., Randerson, J. T., Xu, X., Trumbore, S. E., and Southon, J. R.: Regional patterns of radiocarbon and fossil fuel-derived CO₂ in surface air across North America, *Geophys. Res. Lett.*, 34, L02816, doi:10.1029/2006GL027032, 2007.

5 Hurst, D. F., Lin, J., Romashkin, P. A., Daube, B. C., Gerbig, C., Matross, D. M., Wofsy, S. C., Hall, B. D., and Elkins, J. W.: Continuing global significance of emissions of Montreal Protocol restricted halocarbons in the USA and Canada, *J. Geophys. Res.*, 111, D15302, doi:15310.11029/12005JD006785, 2006.

10 Hurst, D. F., Romashkin, P. A., Elkins, J. W., Oberlander, E., Elansky, N., Belikov, I., Granberg, I., Golitsyn, G., Grisenko, A., Brenninkmeijer, C. A. M., and Crutzen, P. J.: Emissions of ozone-depleting substances in Russia during 2001, *J. Geophys. Res.*, 109, 14303, 2004.

15 Krol, M., Houweling, S., Bregman, B., van den Broek, M., Segers, A., van Velthoven, P. F. J., Peters, W., Dentener, F. J., and Bergamaschi, P.: The two-way nested global chemistry-transport zoom model TM5: algorithm and applications, *Atmos. Chem. Phys.*, 5, 417–432, 2005,
<http://www.atmos-chem-phys.net/5/417/2005/>.

20 Lal, D.: Theoretically expected variations in the terrestrial cosmic-ray production rates of isotopes, in *Proceedings of the International school of Physics, Solar-terrestrial relationships and the Earth environment in the last millennia*, edited by Castagnoli, G. C., 216 pp., North Holland Publishing Company, Amsterdam, 1988.

Levin, I. and Karstens, U.: Inferring high-resolution fossil fuel CO₂ records at continental sites from combined ¹⁴CO₂ and CO observations, *Tellus*, 59B, doi: 10.1111/j.1600-0889.2006.00244.x., 2007.

25 Levin, I. and Kromer, B.: Twenty years of atmospheric ¹⁴CO₂ observations at Schauinsland station, Germany, *Radiocarbon*, 39(2), 205–221, 1997.

Levin, I. and Kromer, B.: The tropospheric ¹⁴CO₂ level in mid-latitudes of the Northern Hemisphere (1959–2003), *Radiocarbon*, 46 (3), 1261–1272, 2004.

30 Levin, I., Kromer, B., Barabase, M., and Munnich, K. O.: Environmental distribution and long-term dispersion of reactor ¹⁴CO₂ around two German nuclear power plants, *Health Physics*, 54(2), 149–156, 1988.

Levin, I., Kromer, B., Schmidt, M., and Sartorius, H.: A novel approach for independent budgeting of fossil fuel CO₂ over Europe by ¹⁴CO₂ observations, *Geophys. Res. Lett.*, 30(23), 2194, 2003.

Eurasian ¹⁴CO₂
measurements

J. C. Turnbull et al.

Title Page

Abstract

Introduction

Conclusions

References

Tables

Figures

◀

▶

◀

▶

Back

Close

Full Screen / Esc

Printer-friendly Version

Interactive Discussion



Eurasian ¹⁴C₂ measurements

J. C. Turnbull et al.

Title Page

Abstract

Introduction

Conclusions

References

Tables

Figures

◀

▶

◀

▶

Back

Close

Full Screen / Esc

Printer-friendly Version

Interactive Discussion



Levin, I., Kromer, B., Schoch-Fischer, H., Bruns, M., Munnich, M., Berndt, D., Vogel, J. C., and Munnich, K. O.: 25 years of tropospheric ¹⁴C observations in central Europe, Radiocarbon, 27, 1–19, 1985.

Magnusson, A., Stenström, K., Skog, G., Adliene, D., Adlyš, G., Hellborg, R., Olariu, A., Zakaria, M., Rääf, C., and Mattsson, S.: Levels of ¹⁴C in the terrestrial environment in the vicinity of two European nuclear power plants, Radiocarbon, 46(2), 863–868, 2004.

Manning, M. R., Lowe, D. C., Melhuish, W. H., Sparks, R. J., Wallace, G., Brenninkmeijer, C. A. M., and McGill, R. C.: The use of radiocarbon measurements in atmospheric sciences, Radiocarbon, 32, 37–58, 1990.

Marland, G., Boden, T. A., and Andres, R. J.: Global, Regional, and National Fossil Fuel CO₂ Emissions, in Trends: A Compendium of Data on Global Change, Carbon Dioxide Information Analysis Center, Oak Ridge National Laboratory, US Department of Energy, Oak Ridge, Tenn., USA, 2003.

Marland, G., Boden, T. A., and Andres, R. J.: Global, regional and national CO₂ emissions, in Trends: A compedium of data on global change, Carbon Dioxide Information Analysis Center, Oak Ridge National Laboratory, US Department of Energy, Oak Ridge, TN, 2006.

Masarik, J. and Beer, J.: Simulation of particle fluxes and cosmogenic nuclide formation in the Earth's atmosphere, J. Geophys. Res., 104(D10), 12 099–13 012, 1999.

Meijer, H. A. J., Smid, H. M., Perez, E., and Keizer, M. G.: Isotopic characterization of anthropogenic CO₂ emissions using isotopic and radiocarbon analysis, Phys. Chem. Earth, 21(5–6), 483–487, 1996.

Montzka, S. A., Myers, R. C., Butler, J. H., Elkins, J. W., and Cummings, S.: Global tropospheric distribution and calibration scale of HCFC-22, Geophys. Res. Lett., 20, 703–706, 1993.

Nakamura, T., Nakazawa, T., Honda, H., Kitagawa, H., Machida, T., Ikeda, A., and Matsumoto, E.: Seasonal variations in ¹⁴C concentrations of stratospheric CO₂ measured with accelerator mass spectrometry, Nucl. Instrum. Methods., B92, 413–416, 1994.

Nydal, R. and Lövseth, K.: Tracing bomb ¹⁴C in the atmosphere 1962–1980, J. Geophys. Res., 88(C6), 3621–3642, 1983.

Olivier, J. G. J. and Berdowski, J. J. M.: Global emissions sources and sinks, in The Climate System, edited by J. Berdowski, R. Guicherit, and B. Heij, Balkema Publishers/Swets and Zeitlinger Publishers, Lisse, The Netherlands, 33–78, 2001.

Olivier, J. G. J., Berdowski, J. J. M., Peters, J., Bakker, J., Visschedijk, A., and Bloos, J.: Applications of EDGAR. Including a description of EDGAR V3.0: reference database with

Eurasian ¹⁴CO₂ measurements

J. C. Turnbull et al.

[Title Page](#)[Abstract](#)[Introduction](#)[Conclusions](#)[References](#)[Tables](#)[Figures](#)[◀](#)[▶](#)[◀](#)[▶](#)[Back](#)[Close](#)[Full Screen / Esc](#)[Printer-friendly Version](#)[Interactive Discussion](#)

trend data for 1970–1995, RIVM, Bilthoven, 2001.

Peters, W., Krol, M. C., Dlugokencky, E. J., Dentener, F. J., Bergamaschi, P., Dutton, G. S., Velthoven, P. v., Miller, J. B., Bruhwiler, L., and Tans, P. P.: Toward regional-scale modeling using the two-way nested global model TM5: Characterization of transport using SF₆, J. Geophys. Res., 109, D19314, doi:10.1029/2004JD005020, 2004.

Potosnak, M. J., Wofsy, S. C., Denning, A. S., Conway, T. J., Munger, J. W., and Barnes, D. H.: Influence of biotic exchange and combustion sources on atmospheric CO₂ concentrations in New England from observations at a forest flux tower, J. Geophys. Res., 104(D8), 9561–9569, 1999.

Prentice, I. C., Farquhar, G. D., Fasham, M., Goulden, M. L., Heimann, M., Jaramillo, V., Ksheshgi, H. S., Le Quere, C., Scholes, R. J., and Wallace, D. W.: The Carbon Cycle and Atmospheric Carbon Dioxide, in Climate Change 2001: Third Assessment Report, 183–237, IPCC, 2001.

Randerson, J., Enting, I. G., Schuur, E. A. G., Caldeira, K., and Fung, I. Y.: Seasonal and latitudinal variability of troposphere Δ¹⁴CO₂: post bomb contributions from fossil fuels, oceans, the stratosphere, and the terrestrial biosphere, Glob. Biogeochem. Cy., 16, 1112, doi:10.1029/2002GB001876, 2002.

Randerson, J. T., Thompson, M. V., Conway, T. J., Fung, I. Y., and Field, C.: The contribution of terrestrial source and sinks to trends in the seasonal cycle of atmospheric carbon dioxide, Glob. Biogeochem. Cy., 11(4), 535–560, 1997.

Rivier, L., Ciais, P., Hauglustaine, D., Bakwin, P. S., Bousquet, P., Peylin, P., and Klonecki, A.: Evaluation of SF₆, C₂Cl₄ and CO as surrogate tracers for fossil fuel CO₂ in the Northern Hemisphere using a chemistry transport model, J. Geophys. Res., 111(D16), D16311, doi:10.1029/2005JD006725, 2006.

Romashkin, P. A., Hurst, D. F., Elkins, J. W., Dutton, G. S., Fahey, D., Dunn, R., Moore, F. L., Myers, R. C., and Hall, B. D.: In situ measurements of long-lived tracer gases in the lower stratosphere by gas chromatography, J. Atmos. Ocean. Tech., 18, 1195–1204, 2001.

Rozanski, K., Levin, I., Stock, J., Falcon, R., and Rubio, F.: Atmospheric (CO₂)-C-14 variations in the Equatorial region, Radiocarbon, 37(2), 509–515, 1995.

Stephens, B. B., Gurney, K. R., Tans, P. P., Sweeney, C., Peters, W., Bruhwiler, L., Ciais, P., Ramonet, M., Bousquet, P., Nakazawa, T., Aoki, S., Machida, T., Inoue, G., Vinnichenko, N., Lloyd, J., Jordan, A., Heimann, M., Shibistowa, O., Langenfelds, R. L., Steele, L. P., Francey, R. J., and Denning, A. S.: Weak northern and strong tropical land carbon uptake from vertical

- profiles of atmospheric CO₂, *Science*, 316, 1732, 2007.
- Stuiver, M. and Polach, H. A.: Discussion: Reporting of ¹⁴C data, *Radiocarbon*, 19(3), 355–363, 1977.
- Takahashi, T., Sutherland, S. C., Sweeney, C., Poisson, A., Metzl, N., Tilbrook, B., Bates, N. R., Wanninkhof, R., Feely, R. A., Sabine, C., Olafsson, J., and Yukihiko, N.: Global sea-air CO₂ flux based on climatological surface ocean pCO₂, and seasonally biological and temperature effects, *Deep Sea Res. II*, 49, 1601–1622, 2002.
- Tans, P. P. and Conway, T. J.: Monthly Atmospheric CO₂ Mixing Ratios from the NOAA CMDL Carbon Cycle Cooperative Global Air Sampling Network, 1968–2002, in *Trends: A Compendium of Data on Global Change*, Carbon Dioxide Information Analysis Center, Oak Ridge National Laboratory, US Department of Energy, Oak Ridge, Tenn., USA, 2005.
- Tarasovaa, O., Brenninkmeijer, C. A. M., Assonov, S., Elansky, N., Rockmann, T., and Brassd, M.: Atmospheric CH₄ along the trans-Siberian railroad (TROIICA) and river Ob: Source identification using stable isotopes, *Atmos. Environ.*, 40(29), 5617–5628, 2006.
- Thompson, M. V. and Randerson, J. T.L Impulse response functions of terrestrial carbon cycle models: method and application, *Glob. Cha. Bio.*, 5, 371–394, 1999.
- Trumbore, S. E.: Potential responses of soil organic carbon to global environmental change, *Proc. Nat. Aca. Sci.*, 94, 8284–8291, 1997.
- Turnbull, J. C., Lehman, S. J., Miller, J. B., Sparks, R. J., Southon, J. R., and Tans, P. P.: A new high precision ¹⁴CO₂ time series for North American continental air, *J. Geophys. Res.*, 112, D11310, doi:11310.11029/12006JD008184, 2007.
- Turnbull, J. C., Miller, J. B., Lehman, S. J., Tans, P. P., Sparks, R. J., and Southon, J. R.: Comparison of ¹⁴CO₂, CO and SF₆ as tracers for determination of recently added fossil fuel CO₂ in the atmosphere and implications for biological CO₂ exchange, *Geophys. Res. Lett.*, 33, L01817, doi:01810.01029/02005GL024213, 2006.
- UNSCEAR, Sources and effects of ionizing radiation, UNSCEAR 2000 report to the General Assembly, with scientific annexes, 1, Annex C, 2000.
- USEPA, Trends in greenhouse gas emissions and sinks: 1990–2002, in EPA 2004 Summary Report GHG emissions inventory 2004, USEPA, 2004.
- Wanninkhof, R.: Relationship between wind-speed and gas-exchange over the ocean, *J. Geophys. Res.*, 97(C5), 7373–7382, 1992.
- Wofsy, S. C., Fan, S.-M., Blake, D., Bradshaw, J., Sandholm, S., Singh, H., Sachse, G., and Harriss, R.: Factors influencing atmospheric composition over subarctic North America dur-

Eurasian ¹⁴CO₂ measurements

J. C. Turnbull et al.

Title Page

Abstract

Introduction

Conclusions

References

Tables

Figures

◀

▶

◀

▶

Back

Close

Full Screen / Esc

Printer-friendly Version

Interactive Discussion



- ing summer, J. Geophys. Res., 99(D1), 1887–0897, 1994.
- Yang, Z., Washenfelder, R., Keppel-Aleks, G., Krakauer, N. Y., Randerson, J. T., Tans, P. P., Sweeney, C., and Wennberg, P.: New constraints on Northern Hemisphere growing season net flux, Geophys. Res. Lett., 34, L12807, doi:10.1029/2007GL029742, 2007.
- 5 Zondervan, A. and Meijer, H. A. J.: Isotopic characterisation of CO₂ sources during regional pollution events using isotopic and radiocarbon analysis, Tellus, 48B, 601–612, 1996.

ACPD

8, 15207–15238, 2008

Eurasian ¹⁴CO₂ measurements

J. C. Turnbull et al.

Title Page

Abstract

Introduction

Conclusions

References

Tables

Figures

◀

▶

◀

▶

Back

Close

Full Screen / Esc

Printer-friendly Version

Interactive Discussion



Eurasian $^{14}\text{CO}_2$
measurements

J. C. Turnbull et al.

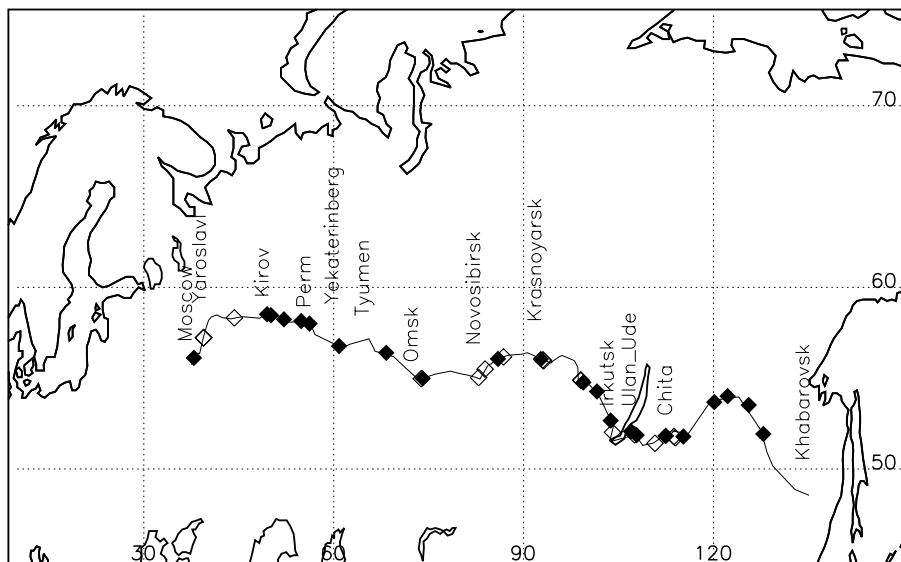


Fig. 1. Map of TROICA flask sampling locations. Closed symbols are samples with CO concentration of less than 250 ppb; these samples were selected for $^{14}\text{CO}_2$ analysis. Open symbols are samples with CO concentration greater than 250 ppb. Major cities and the trans-Siberian railway line are shown for reference.

[Title Page](#)[Abstract](#)[Introduction](#)[Conclusions](#)[References](#)[Tables](#)[Figures](#)[I◀](#)[▶I](#)[◀](#)[▶](#)[Back](#)[Close](#)[Full Screen / Esc](#)[Printer-friendly Version](#)[Interactive Discussion](#)

Eurasian $^{14}\text{CO}_2$
measurements

J. C. Turnbull et al.

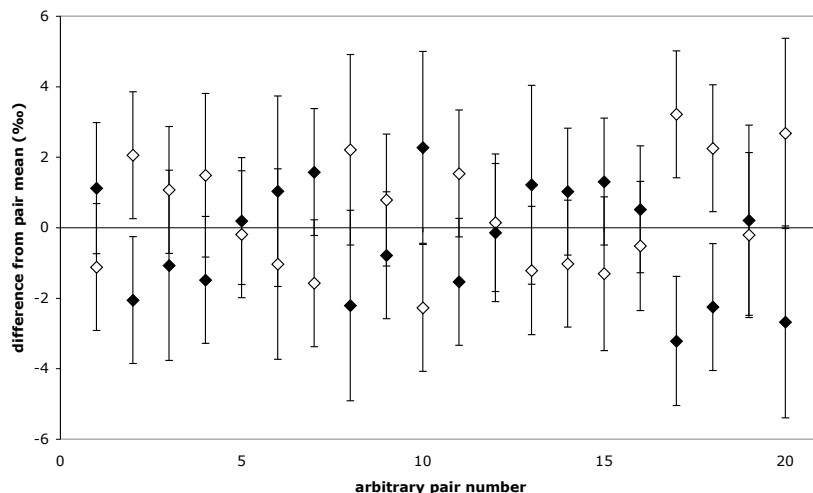


Fig. 2. Pair differences for replicate $\Delta^{14}\text{CO}_2$ measurements. Replicates were obtained by splitting CO_2 extracted from a single whole air sample into two aliquots (each ~ 0.6 mg C). Each aliquot was treated as an individual sample for graphitization and AMS measurement. The difference of each individual measurement from its pair mean is shown. Closed and open symbols are the first and second aliquot taken from each pair, respectively. Error bars are the 1-sigma uncertainty on each measurement.

[Title Page](#)[Abstract](#)[Introduction](#)[Conclusions](#)[References](#)[Tables](#)[Figures](#)[◀](#)[▶](#)[◀](#)[▶](#)[Back](#)[Close](#)[Full Screen / Esc](#)[Printer-friendly Version](#)[Interactive Discussion](#)

Eurasian $^{14}\text{CO}_2$
measurements

J. C. Turnbull et al.

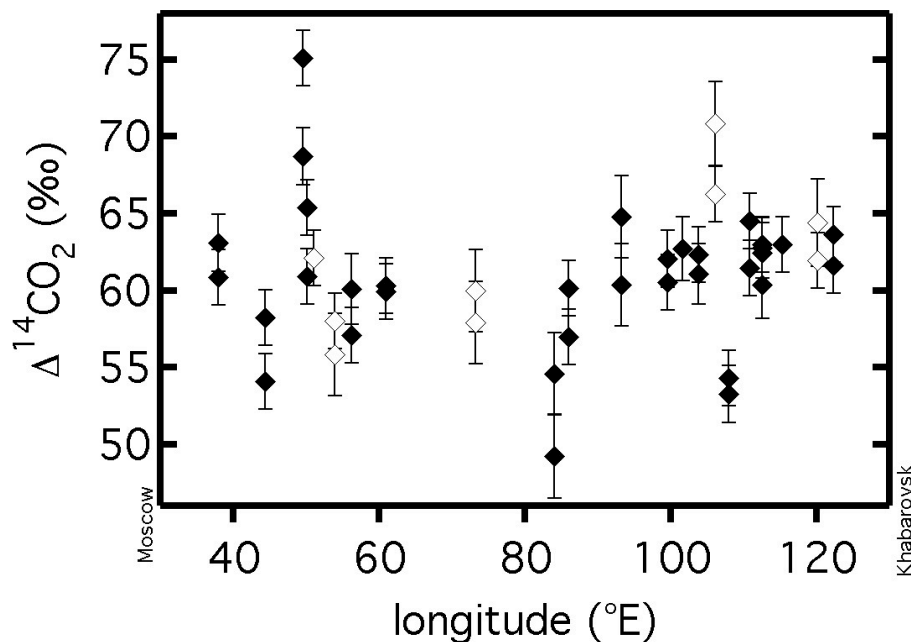


Fig. 3. All $\Delta^{14}\text{CO}_2$ measurements versus longitude. Samples taken during the eastbound journey are shown as solid symbols, westbound samples are open symbols. Error bars are the analytical uncertainty on each measurement.

[Title Page](#)[Abstract](#)[Introduction](#)[Conclusions](#)[References](#)[Tables](#)[Figures](#)[I◀](#)[▶I](#)[◀](#)[▶](#)[Back](#)[Close](#)[Full Screen / Esc](#)[Printer-friendly Version](#)[Interactive Discussion](#)

Eurasian $^{14}\text{CO}_2$
measurements

J. C. Turnbull et al.

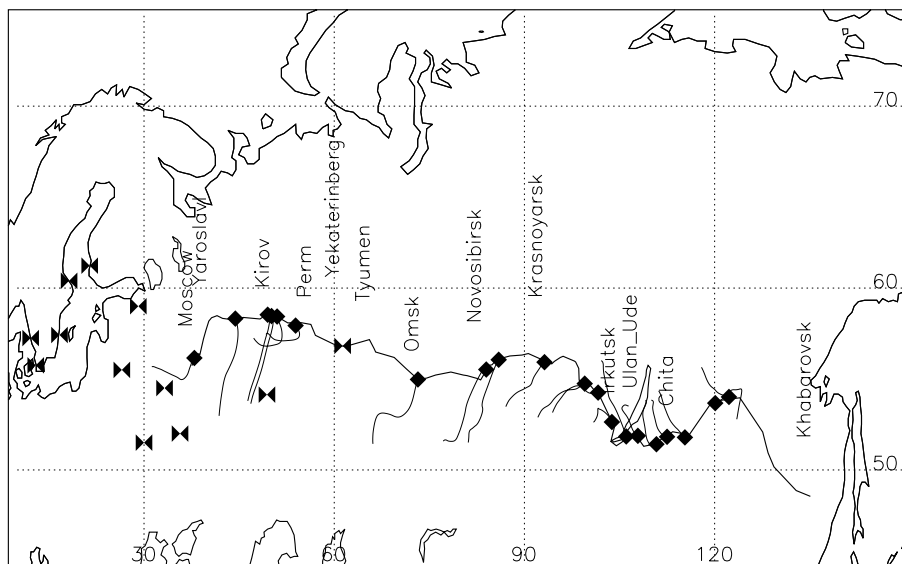


Fig. 4. Sampling locations for TROICA-8 $^{14}\text{CO}_2$ measurements (diamonds). Bow-tie symbols indicate nuclear power plants of types that are known to produce $^{14}\text{CO}_2$ (BWR, FBR or RBMK types) (<http://www.insc.anl.gov/>). Major cities are indicated by name (you may want to put a small x by the location of the city). 48-h back-trajectories for each sampling location and time are shown as thin lines.

Title Page

Abstract

Introduction

Conclusions

References

Tables

Figures

◀

▶

◀

▶

Back

Close

Full Screen / Esc

Printer-friendly Version

Interactive Discussion



Eurasian $^{14}\text{CO}_2$
measurements

J. C. Turnbull et al.

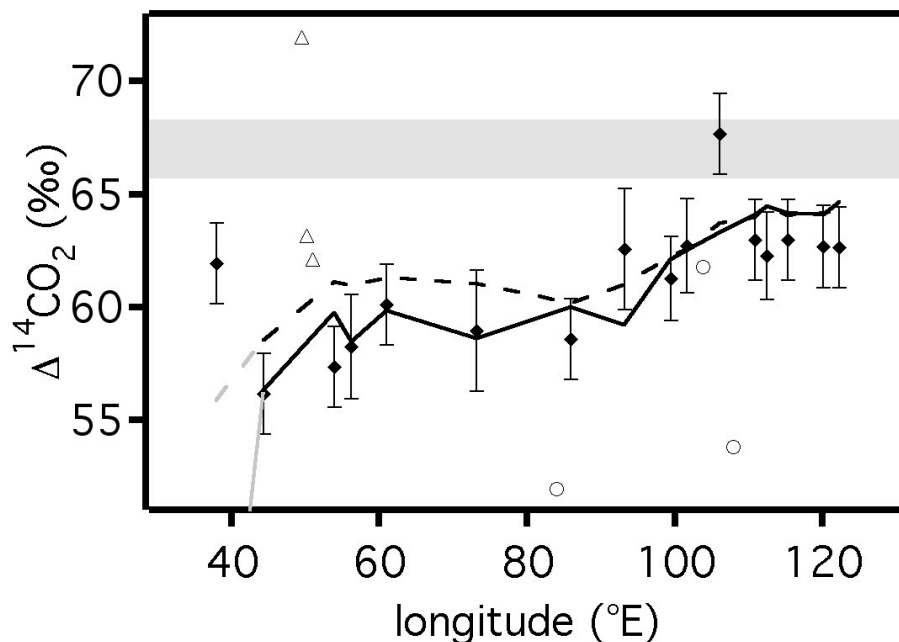


Fig. 5. $\Delta^{14}\text{CO}_2$ as a function of longitude. Closed diamonds are the clean air $\Delta^{14}\text{CO}_2$ dataset. Open symbols indicate samples that may be influenced by either nuclear reactor effluent (triangles) or local city pollution (circles). The shaded bar indicates the NWR $\Delta^{14}\text{CO}_2$ value measured over the same time period and its 1-sigma error envelope. Modeled estimates for each sampling time and location are shown as a solid line (standard mixing) and dashed line (fast mixing). The western-most point in the model estimates, shown in grey, is not used in the analysis (see text).

[Title Page](#)[Abstract](#)[Introduction](#)[Conclusions](#)[References](#)[Tables](#)[Figures](#)[I◀](#)[▶I](#)[◀](#)[▶](#)[Back](#)[Close](#)[Full Screen / Esc](#)[Printer-friendly Version](#)[Interactive Discussion](#)

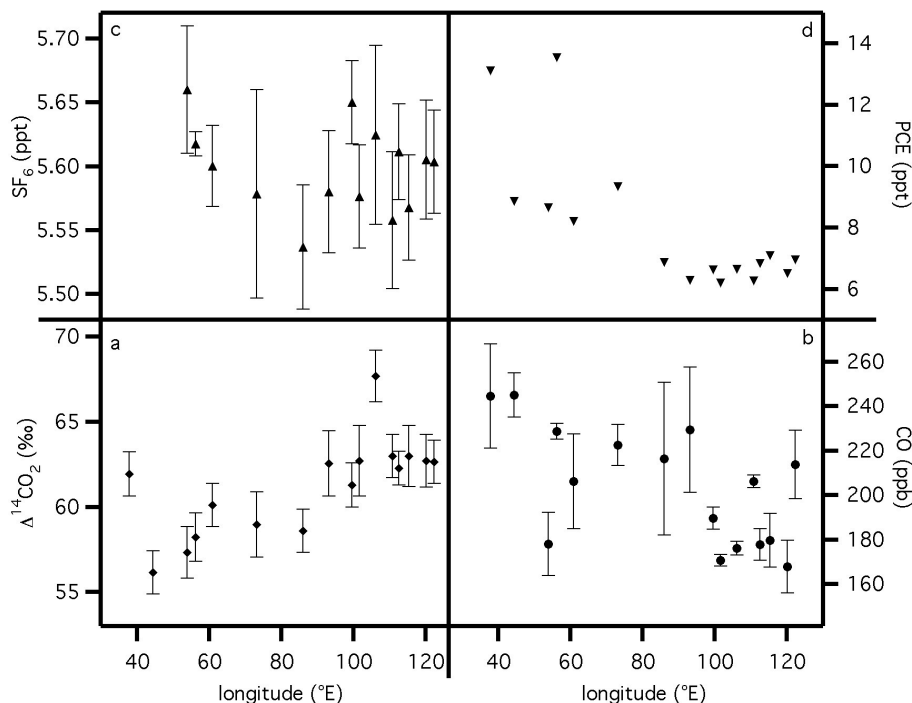


Fig. 6. Comparison of $\Delta^{14}\text{CO}_2$ measurements (panel **a**) with (**b**) ACATS CO measurements from the same time period as flask filling; (**c**) ACATS SF_6 measurements; (**d**) PCE measured in the same flasks. Uncertainties shown are either the measurement uncertainty (PCE and $\Delta^{14}\text{CO}_2$) or the 1-sigma standard deviation of the individual measurements made during the flask filling time (CO and SF_6). The error bars for PCE are smaller than the symbol size. Only the sampling locations considered in the cleaned $\Delta^{14}\text{CO}_2$ dataset are included.

[Title Page](#)[Abstract](#)[Introduction](#)[Conclusions](#)[References](#)[Tables](#)[Figures](#)[◀](#)[▶](#)[◀](#)[▶](#)[Back](#)[Close](#)[Full Screen / Esc](#)[Printer-friendly Version](#)[Interactive Discussion](#)

Eurasian $^{14}\text{CO}_2$
measurements

J. C. Turnbull et al.

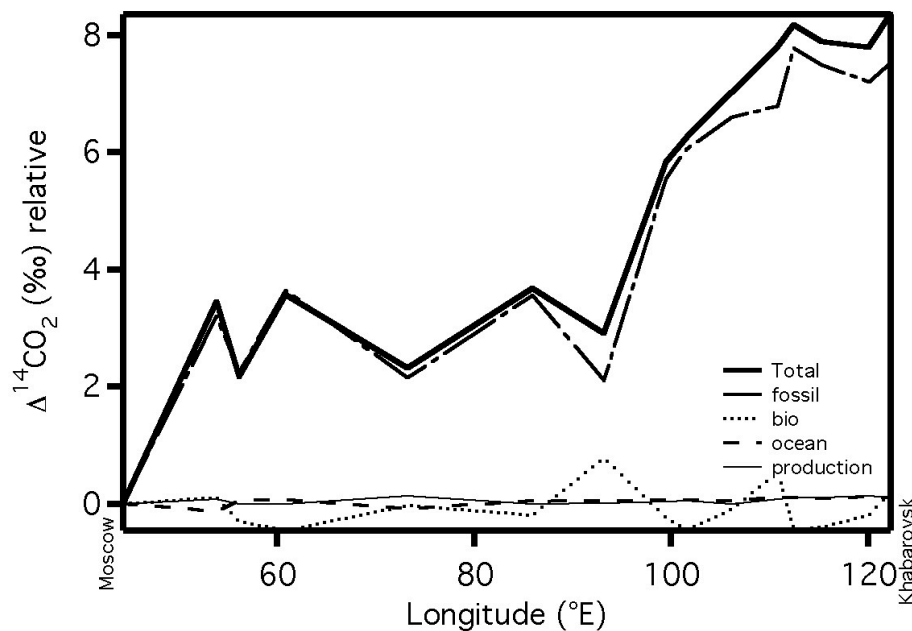


Fig. 7. Contributions of each source to the modeled $\Delta^{14}\text{CO}_2$ gradient using the standard mixing scheme. Each dataset is normalized to have a zero value at the westernmost point.

[Title Page](#)[Abstract](#)[Introduction](#)[Conclusions](#)[References](#)[Tables](#)[Figures](#)[◀](#)[▶](#)[◀](#)[▶](#)[Back](#)[Close](#)[Full Screen / Esc](#)[Printer-friendly Version](#)[Interactive Discussion](#)